THE AMERICAN MINERALOGIST

JOURNAL OF THE MINERALOGICAL SOCIETY OF AMERICA

Vol. 56 JANUARY-FEBRUARY Nos. 1 and 2

THE $Fe^{2+}_3(H_2O)_n(PO_4)_2$ HOMOLOGOUS SERIES: CRYSTAL-CHEMICAL RELATIONSHIPS AND OXIDIZED EQUIVALENTS

PAUL BRIAN MOORE, *Department of the Geophysical Sciences, University of Chicago, Chicago, Illinois 60637.*

ABSTRACT

The atomic arrangements of the known $Fe^{2+}_3(H_2O)_n(PO_4)_2$ homologues are geometrically related and can be considered as progressive octahedral condensations from the higher hydrates to the lower hydrates. Included in the series are vivianite ($n=8$), ludlamite ($n=4$), and phosphoferrite ($n=3$).

Kryzhanovskite is shown to be the oxidized equivalent of phosphoferrite. Its cell formula is approximately $(Fe^{3+}_{7.3}Mn^{2+}_{3.8}Ca_{0.5}Mg_{0.4})$ $((OH)_{7.3}(H_2O)_{4.7})(PO_4)_8$, with $a=9.404$ (16), $b=9.973$ (14), $c=8.536$ (14) Å, space group *Pbna*. Three-dimensional crystal structure analysis led to $R_{hkl}=0.086$ for 530 independent non-zero reflections. The kryzhanovskite (phosphoferrite) atomic arrangement consists of kinked edge-sharing octahedral chains running parallel to the *c*-axis which link by corner-sharing to form sheets parallel to {100}, held together along the *a*-axis by the $(PO_4)^{3-}$ tetrahedra. The octahedrally coordinated cations are strongly ordered, with essentially Fe^{3+} at the inversion center and mixed Fe^{3+}, Mn^{2+} at the general position. A proposed hydrogen-bonding scheme for phosphoferrite involves open tetrahedral geometry.

Heating experiments on vivianite, ludlamite, and phosphoferrite show that only the ferric equivalent of phosphoferrite yields single crystal data indicative of isotypy with the ferrous compound. This phenomenon is explained by local electrostatic neutrality of the $(OH)^-$ ligands in the kryzhanovskite structure which is not possible for the other ferric equivalents. It is suggested that oxidation involves a temperature dependent auto-oxidation-reduction mechanism within the crystal: $2Fe^{2+}(H_2O)^0 \rightarrow 2Fe^{3+}(OH)^- + H_2\uparrow$.

INTRODUCTION

In a series of papers, I have explored the crystal chemistry of members of the hydrated basic iron phosphates (Moore, 1965a, 1965b, 1970a, 1970b, 1970c). These recent investigations, based on three-dimensional crystal structure analyses of key compounds, have brought to light structural interrelationships among many species in this extensive mineral group. Principal factors in their relationships are grounded on the different kinds of octahedral clusters which are stable in crystals. As suggested by Moore (1970c), there appear to be only few predominant kinds of clusters, the great number of species arising from ligand stereoisomerism

TABLE 1. CRYSTAL CELLS OF $Fe^{2+}_3(H_2O)_n(PO_4)_2$–$Fe^{3+}_3(OH)_3(H_2O)_{n-3}(PO_4)_2$–$Mn^{2+}_3(H_2O)_n(PO_4)_2$ MEMBERS

	1	2	3	4	5	6	7
a, Å	9.239 (35)	9.404 (16)	9.462 (18)	9.489 (26)	9.54	10.08	10.541 (5)
b, Å	9.930 (30)	9.973 (14)	10.032 (21)	10.074 (27)	10.08	13.43	4.646 (4)
c, Å	8.453 (26)	8.536 (14)	8.659 (17)	8.601 (31)	8.72	4.70	9.324 (5)
β	—	—	—	—	—	104°30′	100°26 (1)′
V, Å³	775.5 (2.9)	800.5 (1.6)	821.9 (2.1)	822.3 (2.9)	833.0	616.0	449.1
Space group	*Pbna* (possibly *P2na*)					*C2/m*	$P2_1/a$
Z	4					2	2

1. Heated phosphoferrite (P-1′). This is the ferric equivalent of (3).
2. Kryzhanovskite (K-1). Using the analysis of Alekseev in Ginzburg (1950), the formula is $(Fe^{3+}_{7.2}Mn^{2+}_{3.7}Ca_{0.5}Mg_{0.4}((OH)_{7.2}(H_2O)_{4.7})(PO_4)_{8.0}$ based on 8P.
3. Phosphoferrite (P-1). Using analysis 7 in Palache, Berman and Frondel (1951), the formula is $(Fe^{2+}_{8.6}Mn^{2+}_{3.2}Ca_{0.4})(H_2O)_{12.2}(PO_4)_{8.0}$ based on 8P.
4. "Landesite" (L-1). Using the analysis of Berman and Gonyer (1930), the formula is $(Mn^{2+}_{8.4}Fe^{3+}_{3.1}Mg_{1.4}Mn^{3+}_{0.6}Ca_{0.4})(OH, H_2O)_{18.4}(PO_4)_{8.0}$ based 8P. The reported amount of P_2O_5 appears to be low.
5. Reddingite (R-5). Using analysis 5 in Palache, Berman and Frondel, the formula is $(Mn^{2+}_{8.9}Fe^{2+}_{2.9}Fe^{3+}_{0.2}Ca_{0.1}(H_2O)_{12.0}(PO_4)_{8.0}$. This is evidently the unoxidized equivalent of landesite. The cell parameters are from Wolfe (1940).
6. Vivianite. The cell parameters are from Mori and Ito (1950).
7. Ludlamite. The cell parameters are from Abrahams and Bernstein (1966).

about some given cluster. Thus, the large family of fibrous hydrated basic ferrous-ferric phosphates is grounded on the octahedral face-sharing trimer (Moore, 1970a), and many hydrated basic ferric phosphates (and sulfates) appear to be derivative of octahedral corner-sharing chains (Moore, 1970c).

The present study is an attempt to show underlying structural principles within an homologous series, $Fe^{2+}_3(H_2O)_n(PO_4)_2$, where the quantity of water ligands, n, varies in a quantized fashion. Our subject includes three compounds—vivianite, $n=8$; ludlamite, $n=4$; and phosphoferrite, $n=3$. All three compounds occur principally as hydrothermally reworked products of triphylite giant crystals in granite pegmatites and in each species the phosphate ligands are tetradentate and all water molecules are bonded as ligands to the Fe^{2+} cations. In this paper, I shall explore the topological and geometrical relationships among these compounds.

Of further interest is the observation that all three compounds may undergo partial to total oxidation of iron, extending our interest to the series $Fe^{2+}_3(H_2O)_n(PO_4)_2$–$Fe^{3+}_3(OH)_3(H_2O)_{n-3}(PO_4)_2$. This study opens with a detailed account of the kryzhanovskite crystal structure, a species which represents the oxidized equivalent of phosphoferrite.

KRYZHANOVSKITE: ITS CRYSTAL STRUCTURE

Introduction. Kryzhanovskite was first described and named by Ginzburg (1950). It is a rare species whose sole reported locality is the Kalbinsk

pegmatite in the U. S. S.R., where it occurs with sicklerite in association with a highly altered triphylite nodule. Ginzburg proposed the formula $Mn^{2+}Fe^{3+}_2(PO_4)_2(OH)_2 \cdot H_2O$; the poor quality of the crystals, described as monoclinic, prohibited goniometric measurement and establishment of the crystal class.

Through the kindness of Prof. A. S. Povarennykh, I obtained cleavage fragments from a specimen in the Museum of the Academy of Sciences, U.S.S.R. The fragments are deep red-brown in color and display glistening rust-yellow parting surfaces which, under microscopic examination, possess a crinkled appearance. Several fragments proved suitable for single crystal X-ray study which established the relationship of kryzhanovskite with phosphoferrite. This proved most fortunate, since the opportunity was available for the study of the phosphoferrite oxidized equivalent. Accordingly, it was decided to perform a three-dimensional crystal structure analysis on kryzhanovskite.

Although a preliminary account of the phosphoferrite crystal structure was published by Flachsbart (1963), perusal of that paper revealed that aspects of the study were only partially correct. Evidently no further details of that study appeared in print and I concluded that the phosphoferrite structure remained essentially unknown.

Experimental. One fragment proved particularly suitable for single crystal X-ray study. It was broken into several smaller pieces, some of which were ground with Si standard ($a = 5.4301$ Å) and rolled into a 0.2 mm sphere using rubber cement. The calibrated powder data utilized a 114.6 mm diameter Buerger-type camera and Mn-filtered Fe ($K_\alpha = 1.93728$ Å) radiation. The refined cell parameters, obtained initially from the single crystal study, appear in Table 1 and the indexed powder data are offered in Table 2. The powder lines were indexed on the basis of the intensities observed in the single crystal study. Considerable difficulty was encountered in indexing, as many prominent reflections were juxtaposed due to the dimensional similarity among the crystal cell axes.

The single crystal was a platelet exhibiting {001} parting, which measured 0.26×0.16 ×0.10 mm. Preliminary examination included rotation and Weissenberg photography. 2400 reflections were collected on a PAILRED automated diffractometer, using Mo-radiation and a graphite monochromator, a 2.6° half-angle scan with 20 second background measurements on either side of the maxima, and maximum $2\theta = 70°$. These data include the 0 to 10 levels with c as the rotation axis. The data included the symmetry related pairs $I(hkl)$, $I(\bar{h}kl)$ whose integrated intensities were averaged and the $F(obs)$ data obtained by conventional computational procedures, using a local program with optional routines for the PAILRED geometry. The mean error in the intensity averages was 4 percent. The use of Mo radiation, the shape of the crystal, and the relatively low linear absorption coefficient did not necessitate correction for absorption anisotropy. In addition, full 360° ω-scans about the polar (00l) reflections showed that the intensity maxima and minima did not exceed 8 percent of the mean value.

The final $F(obs)$ data included 550 independent "non-zero" reflections which were above the background average and 591 "zero" reflections including the systematic space group absences. Only the "non-zero" data were used in the ensuing analysis.

TABLE 2. KRYZHANOVSKITE POWDER DATA

(Fe/Mn radiation, 114.6 mm camera diameter, silicon standard)

I/I_0	d(*obs*)	d(*calc*)	*hkl*	I/I_0	d(*obs*)	d(*calc*)	*hkl*
4	5.249	5.339	111	4	2.138	2.153	042
7	4.996	4.986	020	2	2.084	2.098	142
5	4.701	4.702	200	2	2.058	2.037	114
5	4.253	4.253	210	3	1.997	2.011	332
4	3.887	3.914	121	2	1.842	1.837	501
2	3.433	3.421	220	2	1.807	1.806	511
10	3.156	3.175	221	2	1.727	1.737	314
2	3.071	3.065	122	3	1.691	1.696	512
3	3.006	3.013	212	3	1.613	1.615	025
2	2.940	2.942	131	2	1.560	1.566	352
5	2.723	2.714	230	2	1.552	1.550	513
4	2.623	2.627	113	5	1.503	1.497	451
5	2.534	2.526	132	2	1.481	1.483	315
1	2.484	2.471	023	3	1.453	1.447	361
4	2.400	2.390	123	1	1.437		
4	2.323	2.319	141	1	1.270		
5	2.207	2.210	411	1	1.132		

Solution of the Structure. Both the film and PAILRED data exhibited systematic absences of the kind $hk0$, $h \neq 2n$; $h0l$, $h+l \neq 2n$; and $0kl$, $k \neq 2n$. Careful search failed to reveal any violations of these systematic absences. Thus, the space group *Pbna* is uniquely determined. This result is not in agreement with Flachsbart's (1963) structure analysis of phosphoferrite, which was based on *P2na*. Although caution must be expressed in assuming phosphoferrites actually crystallize in space group *Pbna*, the conclusion of Flachsbart that the "change in the space group from *Pbna* to *P2na* (my orientation) is caused by the positions of the PO_4 tetrahedra and the H_2O molecules" appears untenable as we shall see in subsequent discussion.

Solution of the kryzhanovskite structure proved straightforward and was initiated from the centrosymmetric average of the coordinate pairs for the Fe and P atoms determined by Flachsbart. Refinement of the coordinates for two Fe and one P in the asymmetric unit led to $R_{hkl}=0.29$. Difference synthesis revealed all the oxygen atoms remaining in the asymmetric unit.

Refinement. Full matrix least-squares atomic coordinate and isotropic thermal vibration parameter refinement proceeded from a local modification of the familiar ORFLS program for the IBM 7094 computer, described by Busing, Martin, and Levy (1962). Scattering curves for Fe^{2+}, P^{3+}, and O^- were prepared from the tables in Mac Gillavry and Rieck (1962). Twenty strong low-angle reflections showing substantial secondary extinction were excluded in the final stages of refinement and the remaining reflections were each given unit weights. Anomalous dispersion corrections were not applied since the only substantial contribution—$+0.9$ for the imaginary dispersion correction of iron—is trivial, compared with the uncertainties associated with the average scattering curves for the octahedral site populations. Convergence was reached at

$$R_{hkl} = \frac{\big|\,|F(obs)| - |F(calc)|\,\big|}{F(obs)} = 0.086.$$

TABLE 3. KRYZHANOVSKITE CELL CONTENTS, ATOMIC COORDINATES AND ISOTROPIC TEMPERATURE FACTORS

(*Errors in parentheses refer to the last digits*)

	M	*x*	*y*	*z*	B(Å²)
Fe(1)	4	0.0000	0.0000	0.0000	0.61 (4)
Fe(2)	8	.4480 (2)	−.1115 (2)	.1367 (2)	.86 (3)
P	8	.7097 (4)	.1032 (4)	.2106 (4)	.42 (5)
O(1) = O_H	4	.4314 (16)	.2500	.0000	1.70 (24)
O(2)	8	.2141 (10)	.2532 (11)	.3273 (11)	.76 (14)
O(3)	8	.1114 (11)	.0336 (10)	.4092 (11)	.95 (15)
O(4)	8	.1573 (11)	.0839 (10)	.1142 (11)	.90 (15)
O(5)	8	.3581 (10)	.0446 (10)	.3027 (11)	.89 (15)
O(6) = O_H	8	.4700 (11)	.3385 (10)	.3631 (13)	1.21 (16)

Further difference synthesis of the three-dimensional data failed to reveal the hydrogen positions, but these distances will be discussed on the basis of geometrical arguments. The atomic coordinate and isotropic thermal vibration parameters are listed in Table 3 and the $|F(obs)| - F(calc)$ data appear in Table 4[1].

Crystal chemistry and interatomic distances. Crystal cell contents calculated from the cell volume in Table 1 and the specific gravity determination and the chemical analysis of O. A. Alekseev in Ginzburg (1950) are presented in Table 5. The results closely conform to the accepted general formula for the phosphoferrite group, that is, $M_3(O_H)_3(PO_4)_2$, where O_H are the oxygen atoms associated with water molecules and hydroxyl groups. Balancing charge by assuming the presence of hydroxyl groups, the cell contents are approximately

$$(Fe^{3+}_{7.3}Mn^{2+}_{3.8}Ca_{0.5}Mg_{0.4})((OH)_{7.3}(H_2O)_{4.7})(PO_4)_8,$$

yielding a calculated water content of 9.2 weight percent which is in fair agreement with 8.75 weight percent obtained by Alekseev. This proposed formula yields a computed density of 3.35 gm/cm³, in good harmony with the specific gravity of 3.31 reported by Ginzburg. Since kryzhanovskite is predominantly the ferric equivalent of the phosphoferrite group, the species has valid status and the name is to apply to all members of the phosphoferrite group containing an excess of 50 mol percent Fe^{3+} in the octahedral sites. The idealized natural end-members in this group are $Fe^{2+}_3(H_2O)_3(PO_4)_2$ (phosphoferrite)-$Fe^{3+}_3(OH)_3(PO_4)_2$ (kryzhanovskite)-$Mn^{2+}_3(H_2O)_3(PO_4)_2$ (reddingite).

[1] To obtain a copy of Table 4, order NAPS Document #01219 from ASIS National Auxiliary Publications Service, c/o CCM Information Sciences, Inc., 22 W. 34th Street, New York, New York 10001; remitting $2.00 for microfiche or $5.00 for photocopies payable to ASIS-NAPS.

TABLE 5. KRYZHANOVSKITE CRYSTAL CELL CONTENTS

	1	2	3			4
CaO	1.50	24.5	0.44			
MnO	16.39	267.6	3.71			
FeO	—	—	—	11.59	ΣM	12.00
MgO	1.36	21.2	0.36			
Fe_2O_3	34.62	565.2	7.08			
P_2O_5	35.30	576.3		8.02	P	8.00
H_2O^+	8.75	142.8				
H_2O^-	0.95	—				
insol.	0.56	—				
	99.37	1597.6				

1. Analysis of Alekseev in Ginzburg (1950).
2. Molecular weight in cell. Computed from volume in Table 1 and specific gravity determination of Ginzburg.
3. Cations in cell.
4. Ideal.

The interesting and important coupled series $Fe^{2+}(H_2O)^0$–$Fe^{3+}(OH)^-$ shall be considered in the ensuing general discussion on the hydrated iron phosphate homologous series but it is appropriate in this section to discuss the interatomic distances. Table 6 presents the polyhedral distances for kryzhanovskite. Numerous crystal structure analyses of related compounds reveal Fe^{3+}–O 1.98 to 2.01 and Mn^{2+}–O 2.18 to 2.23 Å

TABLE 6. KRYZHANOVSKITE POLYHEDRAL DISTANCES[a]

(*Estimated standard errors:* Me-O ±0.01, O-O′ ±0.02 Å)

Fe(1)		*Fe*(2)				*P*	
2 Fe(1)–O(4$_i$)	1.96 Å	1 Fe(2)–O(2)	2.10	1 O(2)–O(6)	2.96	1 P–O(2)	1.47
2 Fe(1)–O(6)	2.01	1 Fe(2)–O(1)	2.13	1 O(1)–O(3)	2.96	1 P–O(5)	1.52
2 Fe(1)–O(5)	2.19	1 Fe(2)–O(6)	2.14	1 O(3)–O(5i)	2.99	1 P–O(3)	1.54
Average:	2.05 Å	1 Fe(2)–O(3)	2.15	1 O(1)–O(2)	3.04	1 P–O(4)	1.59
		1 Fe(2)–O(3i)	2.16	1 O(3)–O(6)	3.13	Average:	1.53
2 O(5)–O(6i)	2.66[b]	1 Fe(2)–O(5i)	2.27	1 O(2)–O(5i)	3.24		
2 O(4)–O(6)	2.73	Average:	2.16	1 O(1)–O(6)	3.24	1 O(2)–O(3)	2.44
2 O(4)–O(6i)	2.88			1 O(2)–O(3i)	3.28	1 O(2)–O(5)	2.44
2 O(4)–O(5i)	2.93	1 O(5i)–O(6)	2.66[b]	1 O(3)–O(5)	3.46	1 O(3)–O(5)	2.49
2 O(4)–O(5)	2.96	1 O(3)–O(3i)	2.69[b]	Average:	3.04	1 O(2)–O(4)	2.50
2 O(5)–O(6)	3.26	1 O(1)–O(3i)	2.85			1 O(4)–O(5)	2.51
Average:	2.90					1 O(3)–O(4)	2.60
						Average:	2.50

[a] i = inversion operation applied to coordinates in Table 3.
[b] Octahedral shared edges.

TABLE 7. KRYZHANOVSKITE ELECTROSTATIC VALENCE BALANCES ABOUT ANIONS (Σ)

			Σ
O(1) = O_H	Fe(2) + Fe(2)	$\frac{2.5}{6}+\frac{2.5}{6}$	0.83
O(2)	P + Fe(2)	$\frac{5}{4}+\frac{2.5}{6}$	1.67
O(3)	P + Fe(2) + Fe(2)	$\frac{5}{4}+\frac{2.5}{6}+\frac{2.5}{6}$	2.08
O(4)	P + Fe(1)	$\frac{5}{4}+\frac{3}{6}$	1.75
O(5)	P + Fe(1) + Fe(2)	$\frac{5}{4}+\frac{3}{6}+\frac{2.5}{6}$	2.17
O(6) = O_H	Fe(1) + Fe(2)	$\frac{3}{6}+\frac{2.5}{6}$	0.92

octahedral averages. It must be concluded from the cell contents and Table 6 that the octahedrally coordinated cations are considerably ordered, with predominant Fe^{3+} in the Fe(1) position with point symmetry $\bar{1}$ and mixed Fe^{3+} and Mn^{2+} at the general Fe(2) position, since the averages are Fe(1)–O 2.05 and Fe(2)–O 2.16 Å respectively. Associated O–O′ octahedral edge distances in Table 6 conform to simple electrostatic arguments since the octahedral shared edges are the shortest distances for their polyhedra.

Likewise, the electrostatic valence balance calculations in Table 7 further explain the interatomic distances. From the cell contents and the average Fe–O distances, the formal charge on Fe(1) is *ca.* +3, and Fe(2) is *ca.* +2.5. Hence, O(2), with $\sum=1.67$ is the most undersaturated of the anions and affords the shortest Me–O distances, *i.e.*, Fe(2)–O(2) 2.10 Å and P–O(2) 1.47 Å, the latter an unusually short distance for P^{5+}–O. The most oversaturated anion, O(5) with $\sum=2.17$, possesses considerably longer octahedral distances than average: Fe(1)–O(5) 2.19 Å and Fe(2)–O(5) 2.27 Å. For the anions which are nearly neutral, compensation occurs, for if P–O is long Fe–O is short and *vice versa*. These arguments, along with the observed isotropic thermal vibration parameters which indicate fully occupied anion positions, substantiate charge balance through the substitution of hydroxyl groups for water molecules since the substitution of O^{2-} for H_2O would leave voids in the structure. Further discussion on the relative stabilities of the structures of the oxidized hydrated iron phosphate homologues appears in the next section.

Flachsbart's (1963) Fe–O interatomic distances for phosphoferrite, which range from 2.10 to 3.26 Å, appear to be in error. Unfortunately, no mention is made of the data collection and further study on phosphoferrite will be necessary if accurate interatomic distances are to be obtained for that species.

General Crystal Chemistry of the $Fe^{2+}_3(H_2O)_n(PO_4)_2$ Homologues

Topology. The atomic arrangements of the three homologues, vivianite, ludlamite, and phosphoferrite (kryzhanovskite) are known. Each structure may be conceived as a denser condensation of octahedral clusters of its higher hydrates. The octahedral cluster formulae for the three species can be written on the basis of $M_r\phi_s$, where ϕ are the vertices, s of which are associated with the r M-octahedra. In vivianite $M_r\phi_s = Fe_3\phi_{16}$, where $\phi_{16} = 8\ O_P + 8\ O_H$, with O_P = phosphate oxygen and O_H = water oxygen. For ludlamite $M_r\phi_s = Fe_3\phi_{12}$, where $\phi_{12} = 8\ O_P + 4\ O_H$; and for phosphoferrite $M_r\phi_s = Fe_3\phi_{11}$, where $\phi_{11} = 8\ O_P + 3\ O_H$.

For all these structures, appropriate projections yield a striking relationship. This relationship can be seen in the polyhedral diagrams for vivianite, ludlamite, and kryzhanovskite (phosphoferrite) in Figures 1, 2, and 3 respectively. The cell criteria for ludlamite and vivanite appear in Table 1 for comparative purposes. Projections down the vivianite c^*, the ludlamite b^* and the kryzhanovskite a^* axes show similarity in the orientations of the octahedra and tetrahedra. Locally, these orientations approximate fragmented hexagonal close-packed units or strips, with the axes of projection normal to the close-packed oxygen layers. These three compounds are not truly close-packed since it is not possible topologically to continuously deform the polyhedra into ideal closest packings without breaking and rearranging some bonds. Since the systems are not topologically close-packed, they will be called *interrupted close-packings*. The orientations of the interrupted close-packed layers reflect similarities in the translations normal to these layers: $c \sin\beta)_{viv} \sim b)_{lud} \sim a/2)_{kry} \sim 4.7$ Å, which is the typical repeat distance for a hexagonal close-packed oxygen framework.

Accordingly, the homologous series can be conceived as a progressive condensation of octahedral clusters, from open clusters in the high hydrate to sheets in the lower hydrates. The vivianite structure, investigated by Mori and Ito (1950), consists of insular octahedral edge-sharing doublets and insular singlets joined to form slabs perpendicular to the b-axis by the $(PO_4)^{3-}$ tetrahedra (Fig. 1). In ludlamite, further fusion occurs, with the appearance of octahedral edge-sharing linear triplets corner-linked to similar triplets, forming somewhat open trellises oriented

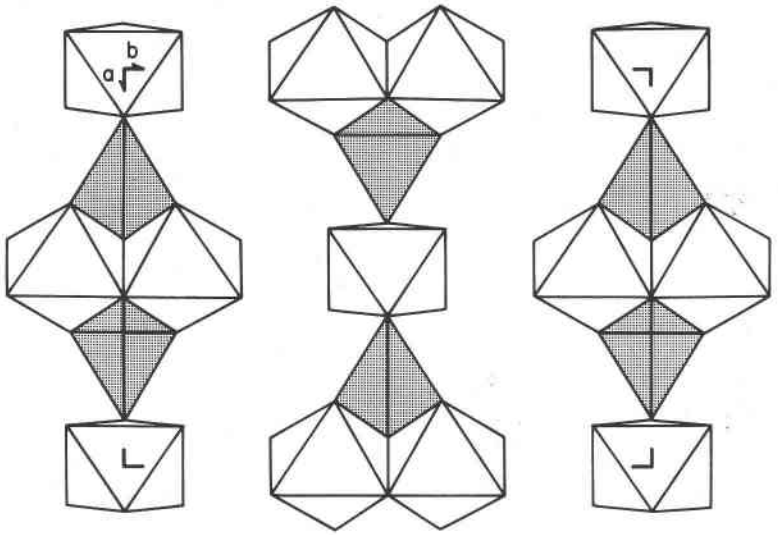

FIGS. 1–3. Polyhedral diagrams of the vivianite, ludlamite and kryzhanovskite atomic arrangements.

FIG. 1. Vivianite projected down the z^*-axis. The tetrahedra are stippled and connect to octahedral levels above and below. The coordinates are from Mori and Ito (1950).

parallel to $\{\bar{1}02\}$. The trellises are linked to each other by the $(PO_4)^{3-}$ tetrahedra oriented in a fashion similar to vivianite (Fig. 2). The ludlamite structure was first investigated by Ito and Mori (1951) and refined with high accuracy by Abrahams and Bernstein (1966) as part of a detailed neutron diffraction study. The kryzhanovskite (phosphoferrite) structure, Fig. 3, consists of infinite kinked edge-sharing octahedral chains which link at free corners to form sheets oriented parallel to $\{100\}$. These sheets are connected along the a-axis by the bridging $(PO_4)^{3-}$ tetrahedra which are oriented akin to vivianite and ludlamite.

The geometrical relationships among members of this homologous series are clearly evident. It was stated elsewhere (Moore, 1970b) that the controlling factor in the paragenesis of such compounds is the relative stability of water ligands with respect to temperature. With increasing temperature, a series of "condensation" reactions take place, the stepwise loss of water resulting in the fusion of more open octahedral clusters to form more condensed arrangements. Analogously, with decreasing temperature the reverse would be true; as water ligands increase in quantity in the structures, more open arrangements appear. This accounts

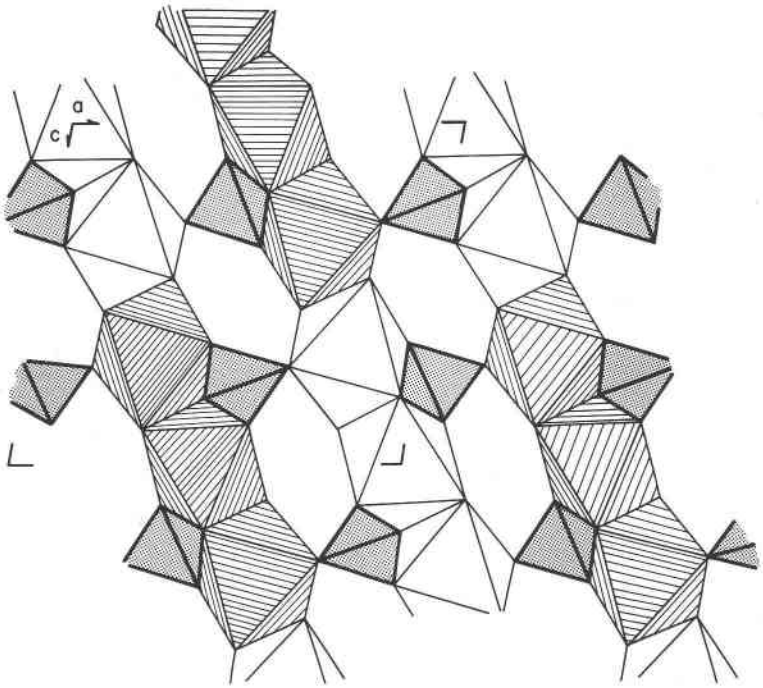

FIG. 2. Ludlamite projected down the y-axis. The octahedral edge-sharing triplets at $y=1/2$ are ruled. The tetrahedra, which link to octahedral levels above and below are stippled. The coordinates are from Abrahams and Bernstein (1966).

for the fact that phosphoferrite is usually the earliest-formed member of the series, postdated by ludlamite which in turn is postdated by vivianite. Such sequences can be seen in specimens collected from hydrothermally reworked triphylite pods, such as at the Palermo #1 mine, North Groton, New Hampshire; Bull Moose pegmatite, Keystone, South Dakota; and Hagendorf Süd, Bavaria.

It would be instructive to attempt synthesis of compounds in this homologous series. So far, only vivianite, ludlamite, and phosphoferrite appear to be the three known compounds. However, no detailed synthesis has ever been made, nor has any detailed study been undertaken on the myriads of hydrothermally reworked products of triphylite. It is quite likely that other members of the series still remain to be discovered.

HYDROGEN BONDING

Although there exist geometrical relationships among the vivianite, ludlamite, and kryzhanovskite (phosphoferrite) structures, there do not

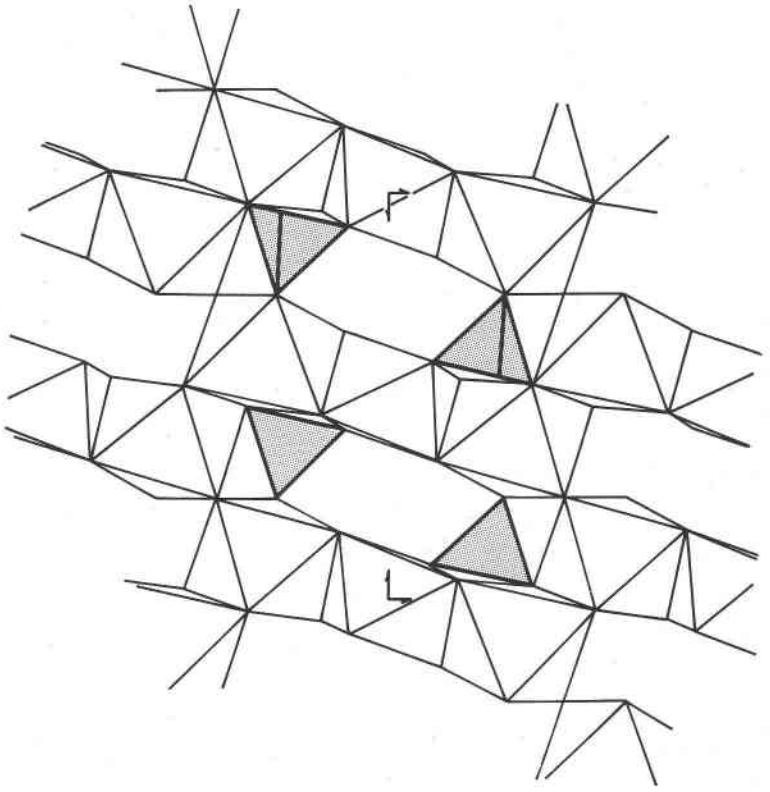

FIG. 3. Kryzhanovskite projected down the x-axis showing the octahedral sheets and the connecting tetrahedra (stippled).

appear similar relationships in their hydrogen bonding schemes. It is only possible to offer a qualitative discussion since the vivianite structure is approximately known and since kryzhanovskite possesses most of the octahedral cations in the trivalent state. Abrahams and Bernstein (1966) presented relatively accurate hydrogen positions for ludlamite which they obtained from careful X-ray and neutron diffraction studies. Ludlamite remains the only structure where the hydrogen bonds are known, quantitatively as well as qualitatively, with sufficient accuracy.

Figures 4, 5, and 6 show the probable hydrogen bonding schemes for the three species. These figures can be superimposed upon the polyhedral diagrams in Figure 1, 2, and 3. The O–H . . . O bond is represented as an arrow whose head points in the direction of the oxygen atom accepting the hydrogen bond and whose tail is situated at the oxygen atom of the water molecule. According to Abrahams and Bernstein, the O . . . O

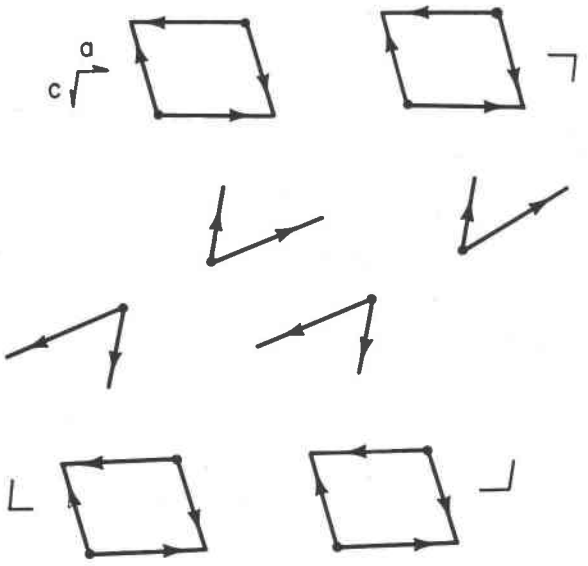

FIGS. 4–6. Probable hydrogen bonds in ludlamite, vivianite and kryzhanovskite. These diagrams can be superimposed on the Fig. 1 series. The tails of the arrows are centered on the water oxygen and the heads point to the hydrogen acceptors.

FIG. 4. Arrangement in ludlamite.

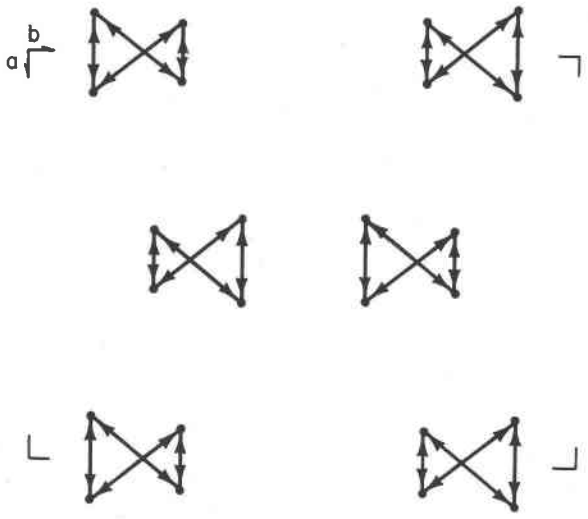

FIG. 5. Arrangement in vivianite.

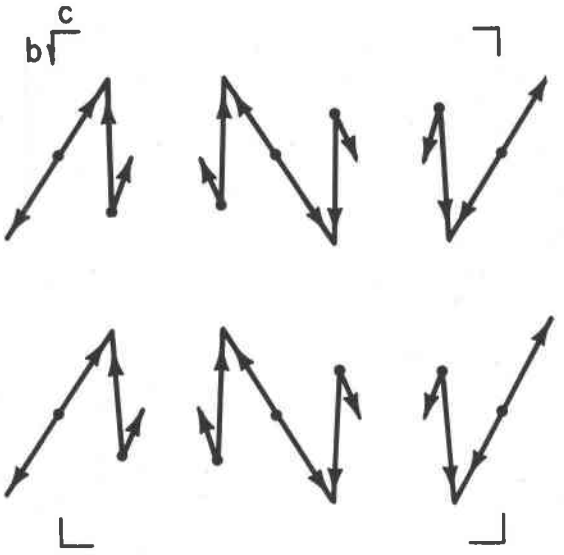

FIG. 6. Arrangement in kryzhanovskite.

distances in ludlamite are relatively short, ranging from 2.541 (3) to 2.750 (3) Å. Three of the four $(PO_4)^{3-}$ oxygen atoms are receptors of hydrogen bonds, with one oxygen atom receiving two such bonds. The resulting network in ludlamite (Fig. 4) consists of a rhombus-like outline and insular bonds, both geometries of which are tilted away from the *xz*-plane. In this manner, the bonds link between populated octahedral levels.

The geometry of the vivianite structure leads to a probable hydrogen bonding scheme which can be represented as a closed tetrahedron (Fig. 5), distinct from ludlamite in that all the receptors of the bonds are water molecules. These bonds are situated between the octahedral levels and are the only chemical bonds which are broken by the perfect $\{010\}$ cleavage in vivianite crystals. Geometrically, it does not appear possible to select bonds which accept oxygen atoms associated with the $(PO_4)^{3-}$ tetrahedra.

The probable hydrogen bonding scheme for kryzhanovskite, and possibly phosphoferrite, in Figure 6 is based on an open tetrahedron. Some of these bonds link between the octahedral levels. This scheme involves two of the four $(PO_4)^{3-}$ oxygen atoms, with O(4) accepting two bonds. The shortest distance, 2.57(2) Å, is between O(2) . . . O(6). The remaining distances, O(6) . . . O(4) 3.10 (2) and O(1) . . . O(4) 3.21 (2) Å, are considerably longer than typical distances in inorganic salts

involving water molecules. It must be stressed, however, that the oxidized nature of kryzhanovskite would lead to substantial disorder in the O–H . . . O bonds, especially for O(1) and these distances may differ substantially from those occurring in unoxidized phosphoferrite.

Of the three structures, only vivianite possesses hydrogen bonds which are necessary components in the rigidity of the crystal structure since both phosphoferrite and ludlamite involve three-dimensional linkages of . . . *M*–O–P–O . . . bonds. As discussed in the next section, this difference may contribute in part to the instability of vivianite crystals upon progressive oxidation of the iron.

Oxidation Sequences

Vivianite, ludlamite, and phosphoferrite are known to undergo rapid oxidation at low temperature in the presence of air. Accordingly, crystals of vivianite and ludlamite from the Palermo #1 mine, and phosphoferrite from Hagendorf Süd were heated in air at 120°C, 180°C, and 240°C for five days in open capillaries calibrated with a chromel alumel thermocouple in contact with the crystals. The products were then quenched to room temperature, dissolved in cold HCl solution, and titrated against potassium dichromate solutions. Ludlamite at 120°C and 180°C was only superficially oxidized and yielded identical powder patterns as the starting material. At 240°C, the product proved to consist of iron in the ferric state only, but the powder lines were diffuse and totally unrelated to the starting material. Vivianite at all three temperatures was totally oxidized to essentially amorphous material. On the other hand, phosphoferrite heated at 240°C was oxidized to its ferric equivalent and yielded superior single crystal and powder photographs which indicated isotypy with the ferrous material. The only difference was considerable line and spot broadening in the oxidized materials.

Figure 7 presents available analyses and the results of the heating experiments on the phosphoferrite-kryzhanovskite-reddingite series. Unheated phosphoferrite is labelled P-1, its oxidized equivalent P-1′; kryzhanovskite is labelled K-1. The available analyses of reddingite (Palache, Berman, and Frondel, 1951), labelled R-1 to R-5, are also included. Finally, "landesite", properly a ferrian reddingite according to Moore (1964), is designated L-1. Cell parameters for P-1, P-1′, K-1, and L-1 are given in Table 1; they are based on single crystal studies and the refined powder data using the indices obtained for kryzhanovskite. The cell parameters for landesite reported by Moore (1964) are modified as a result of more complete and corrected Miller indices derived from the kryzhanovskite three-dimensional single crystal data. The crystal cell volumes are dependent on the relative states of oxidation, with the cell

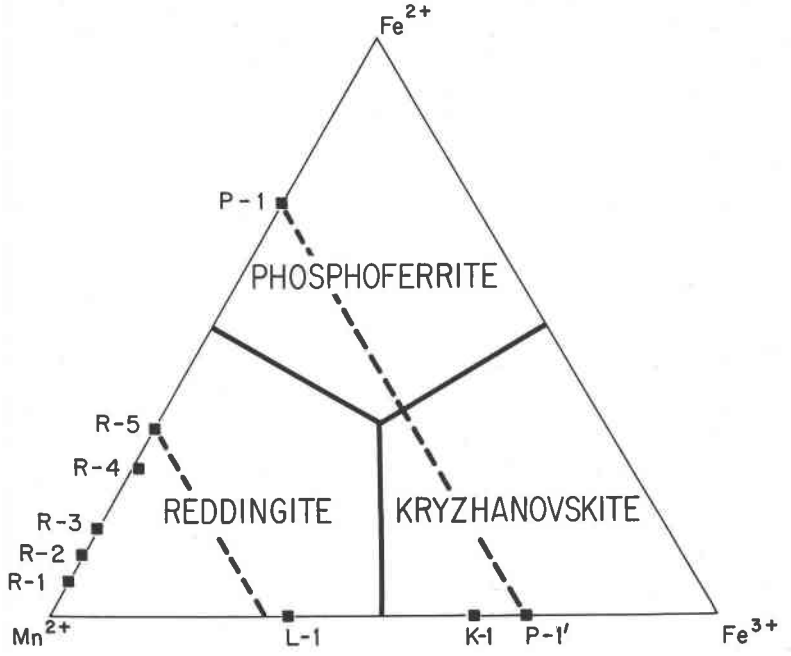

FIG. 7. Triangular diagram of the phosphoferrite (Fe^{2+})-kryzhanovskite (Fe^{3+})-reddingite (Mn^{2+}) end-members. Compositions are plotted as mol fractions of the end-members. R-1 to R-5 refer to reddingite analyses 1 to 5 in Palache, Berman and Frondel (1951), L-1 is the composition of "landesite" (the oxidized equivalent of R-5), K-1 is kryzhanovskite, P-1 is phosphoferrite from Hagendorf Süd and P-1′ is its oxidized equivalent.

volume decreasing with increasing iron oxidation grade. The relationships among the cell volumes are consistent with the crystal radii $Mn^{2+} > Fe^{2+} > Fe^{3+}$, which are the only major octahedrally coordinated cations in Figure 7 and whose relative proportions in the crystal can be obtained from this figure. With the exception of powder line broadening for the ferric members, these compounds appear to be crystallographically isostructural.

Why should the oxidized equivalent of phosphoferrite exist as a "stable" crystal whereas the oxidized equivalents of vivianite and ludlamite are structurally unstable? The explanation appears to lie in the criteria necessary for local electrostatic neutrality of the anions about cations. In ludlamite, vivianite, and phosphoferrite, crystal structure analysis has established that all water molecules are bonded as ligands to the octahedrally coordinated iron atoms. In vivianite, the water molecules are each associated with one iron atom. Thus, the hypothetical ferric end-member, written $Fe^{3+}_3(OH)_3(H_2O)_5(PO_4)_2$, is unstable since

OH^- are severely undersaturated electrostatically with respect to Fe^{3+}. No example is known of OH^- only coordinated to a single Fe^{3+} cation. Additional instability is probably induced through the breakdown of hydrogen bonds which are essential for structural rigidity. Indeed, oxidized vivianites characteristically show a flaky appearance parallel to {010}.

In ludlamite, each water molecule is associated with two iron atoms. Writing the hypothetical oxidized equivalent as $Fe^{3+}_3(OH)_3(H_2O)(PO_4)_2$, the H_2O molecule remaining is severely oversaturated and consequently the crystal is unstable. The oxidized equivalent of phosphoferrite, which is $Fe^{3+}_3(OH)_3(PO_4)_2$, is essentially neutral since each hydroxyl group is bonded to two Fe^{3+} cations in octahedral coordination.

Analogous to vivianite, progressive oxidation of Fe^{2+} in phosphoferrite should lead to dark green to blue color. Since phosphoferrite consists of edge-sharing octahedral chains oriented parallel to the *c*-axis, homonuclear mixed-valence electron transfer would result in strong absorption by the crystal parallel to {001}. Finally, the pure ferric equivalent, like the ferrous compound, would appear relatively weakly pleochroic, in contrast with crystals possessing iron in mixed valence states.

What is the mechanism accounting for progressive oxidation of phosphoferrite? The most likely is one of auto-oxidation-reduction by cleavage of protons from the water ligands, forming hydroxyl groups and ferric iron, that is, $2Fe^{2+}(H_2O)^0 \rightarrow 2Fe^{3+}(OH)^- + H_2\uparrow$. A test for the existence of such a mechanism would involve heating phosphoferrite in anaerobic environments and quantitatively collecting hydrogen.

Regarding kryzhanovskite, it is reasonable to state that the compound is formed by oxidation of parent phosphoferrite but it is uncertain whether or not kryzhanovskite is thermodynamically stable since it has not been synthesized directly from ferric salts. Evidently, the temperature of kryzhanovskite formation was too low for the oxidation of Mn^{2+}: it is generally observed that Fe^{2+} oxidizes before Mn^{2+} in mineral crystals containing both cations in solid solution.

ACKNOWLEDGMENTS

The study of a natural oxidized equivalent of phosphoferrite was made possible through the generous contribution of type kryzhanovskite by Prof. A. S. Povarennykh. Prof. D. J. Fisher supplied the phosphoferrite specimen from Hagendorf Süd.

Financial assistance throughout this study was supplied by an Advanced Research Projects Agency grant administered to the University of Chicago and the NSF GA10932 research grant.

REFERENCES

ABRAHAMS, S. C., AND J. L. BERNSTEIN (1966) Crystal structure of paramagnetic ludlamite, $Fe_3(PO_4)_2 \cdot 4H_2O$ at 209°K. *J. Chem. Phys.* **44**, 2223–2229.

BERMAN, H., AND F. A. GONYER (1930) Pegmatite minerals of Poland, Maine. *Amer. Mineral.* **15**, 375–386.

BUSING, W. R., K. O. MARTIN, AND H. A. LEVY (1962) ORFLS, a Fortran crystallographic least-squares program. *U. S. Clearinghouse Fed. Sci. Tech. Info. Rep.* **ORNL-TM-305**.

FLACHSBART, I. (1963) Zur Kristallstruktur von Phosphoferrit, $(Fe, Mn)_3(PO_4)_2 \cdot 3H_2O$. *Z. Kristallogr.* **118**, 327–331.

ITO, T., AND H. MORI (1951) The crystal structure of ludlamite. *Acta Crystallogr.* **4**, 412–416.

MAC GILLAVRY, C. H., AND G. D. RIECK, eds. (1962) *International Tables for X-ray Crystallography*, **Vol. 3**., The Kynoch Press, Birmingham, England.

MOORE, P. B. (1964) Investigations of landesite. *Amer. Mineral.* **49**, 1122–1125.

——— (1965a) The crystal structure of laueite. *Amer. Mineral.* **50**, 1884–1892.

——— (1965b) A structural classification of Fe-Mn orthophosphate hydrates. *Amer. Mineral.* **50**, 2052–2062.

——— (1970a) Crystal chemistry of the basic iron phosphates. *Amer. Mineral.* **55**, 135–170.

——— (1970b) A crystal-chemical basis for short transition series orthophosphate and orthoarsenate parageneses. *Neues Jahrb. Mineral. Monatsh.* **1970**, 39–44.

——— (1970c) Structural hierarchies among minerals containing octahedrally coordinating oxygen. I. Stereoisomerism among corner-sharing octahedral and tetrahedral chains. *Neues Jahrb. Mineral. Monatsh.*, **1970**, 163–173.

MORI, H., AND T. ITO (1950) The crystal structures of vivianite and symplesite. *Acta Crystallogr.* **3**, 1–6.

PALACHE, C., H. BERMAN, AND C. FRONDEL (1951) *The System of Mineralogy*, **Vol. 2**, 7th Ed., John Wiley & Sons, New York, 727–731.

WOLFE, C. W. (1940) Classification of minerals of the type $A_3(XO_4)_2 \cdot n\,H_2O$. *Amer. Mineral.* **25**, 738–753.

Manuscript received, June 16, 1970; accepted for publication, October 14, 1970.